

Role of spin-orbit coupling in the alloying behavior of multilayer $\text{Bi}_{1-x}\text{Sb}_x$ solid solutions revealed by a first-principles cluster expansion

A. Ektarawong ^{1,2,*}, T. Bovornratanaraks,^{1,2} and B. Alling ³

¹*Extreme Condition Physics Research Laboratory, Physics of Energy Materials Research Unit, Department of Physics, Faculty of Science, Chulalongkorn University, Bangkok 10330, Thailand*

²*Thailand Center of Excellence in Physics, Ministry of Higher Education, Science, Research and Innovation, 328 Si Ayutthaya Road, Bangkok 10400, Thailand*

³*Theoretical Physics Division, Department of Physics, Chemistry and Biology (IFM), Linköping University, SE-581 83 Linköping, Sweden*



(Received 8 November 2019; revised manuscript received 18 March 2020; accepted 24 March 2020; published 13 April 2020)

We employ a first-principles cluster-expansion method in combination with canonical Monte Carlo simulations to study the effect of spin-orbit coupling on the alloying behavior of multilayer $\text{Bi}_{1-x}\text{Sb}_x$. Our simulations reveal that spin-orbit coupling plays an essential role in determining the configurational thermodynamics of Bi and Sb atoms. Without the presence of spin-orbit coupling, $\text{Bi}_{1-x}\text{Sb}_x$ is predicted to exhibit at low-temperature chemical ordering of Bi and Sb atoms, leading to formation of an ordered structure at $x \approx 0.5$. Interestingly, the spin-orbit-coupling effect intrinsically induced by the existence of Bi and Sb results in the disappearance of chemical ordering of the constituent elements within an immiscible region existing at $T < 370$ K, and consequently $\text{Bi}_{1-x}\text{Sb}_x$ displays merely a tendency toward local segregation of Bi and Sb atoms, resulting in coexistence of Bi-rich and Sb-rich $\text{Bi}_{1-x}\text{Sb}_x$ solid solutions without the formation of any ordered structure of $\text{Bi}_{1-x}\text{Sb}_x$ as predicted in the absence of spin-orbit coupling. These findings distinctly highlight an influence of spin-orbit coupling on the alloying behavior of $\text{Bi}_{1-x}\text{Sb}_x$ and probably other alloys composed of heavy elements, where the spin-orbit-coupling effect is supposed to be robust.

DOI: [10.1103/PhysRevB.101.134104](https://doi.org/10.1103/PhysRevB.101.134104)

I. INTRODUCTION

Since the past few decades, substitutional alloys, composed of antimony (Sb) and bismuth (Bi) and denoted by $\text{Bi}_{1-x}\text{Sb}_x$, have constantly received attention from many researchers, resulting in extensive studies of the $\text{Bi}_{1-x}\text{Sb}_x$ from experimental and theoretical points of view [1–18]. One of the reasons can be attributed to their unique thermoelectric and electronic properties, making $\text{Bi}_{1-x}\text{Sb}_x$ a promising candidate for thermoelectric applications [1–6,9–11]. Under ambient conditions, $\text{Bi}_{1-x}\text{Sb}_x$ crystallizes in the rhombohedral $A7$ -type structure with the space group of $R\bar{3}m$, which is isostructural to those of its constituents. For this particular case, Bi and Sb atoms form buckled sheets with an ABC vertical stacking sequence, as visualized by Fig. 1(a) [2,19]. Owing to rather weak interactions coupling between the buckled sheets, a single layer or a few layers of $\text{Bi}_{1-x}\text{Sb}_x$ can in principle be achieved by using exfoliation methods [20,21] and epitaxial growth [22–25]. As shown by several independent studies, a monolayer of $\text{Bi}_{1-x}\text{Sb}_x$ can, apart from its intriguing thermoelectric properties, behave as a topological insulator, when the material is subjected to biaxial strain larger than $\sim 14\%$ [26], and exhibit giant Rashba spin splitting in its electronic band structure because of a robust spin-orbit-coupling (SOC) effect induced particularly by Bi atoms [15,16]. The rise

of both topological states and Rashba spin splitting in the electronic structure in a single layer of $\text{Bi}_{1-x}\text{Sb}_x$ has provided opportunities for utilizing $\text{Bi}_{1-x}\text{Sb}_x$ as a substance to fabricate two-dimensional material-based optoelectronic and spintronic devices [7,8,14–16]. This consequently has given rise to further interest in $\text{Bi}_{1-x}\text{Sb}_x$.

In the case of bulk/multilayer $\text{Bi}_{1-x}\text{Sb}_x$, it is generally accepted that, at $T \gtrsim 450$ K, Bi and Sb readily form a continuous series of disordered solid solutions over the entire composition range, where $0 \leq x \leq 1$ [27,28], while information on its alloying behavior at lower temperature, to the best of our knowledge, has up to now been left undisclosed. This may be interpreted by slow atomic mobility of Bi and Sb atoms at low temperature, preventing $\text{Bi}_{1-x}\text{Sb}_x$ to reach its actual equilibrium states in experiment. Nevertheless, it was recently demonstrated that $\text{As}_{1-x}\text{Sb}_x$ solid solutions, which are also the group-V element-based alloys and behave similarly to $\text{Bi}_{1-x}\text{Sb}_x$ in terms of crystal structure formation, can display chemical ordering of As and Sb atoms to form an $A7$ -type ordered and stoichiometric compound of AsSb at $T < 475$ K [29,30]. Such discovery in the binary As-Sb system has given rise to a curiosity, whether or not $\text{Bi}_{1-x}\text{Sb}_x$ could also display chemical ordering and/or clustering of Bi and Sb atoms at $T < 450$ K, analogous to $\text{As}_{1-x}\text{Sb}_x$. In this regard, it is worth emphasizing that, in general, the properties of any alloy system not only vary with the relative content of the alloy constituents, but they also depend on the atomic configuration of the constituents, i.e., how the constituent

*Annop.E@chula.ac.th

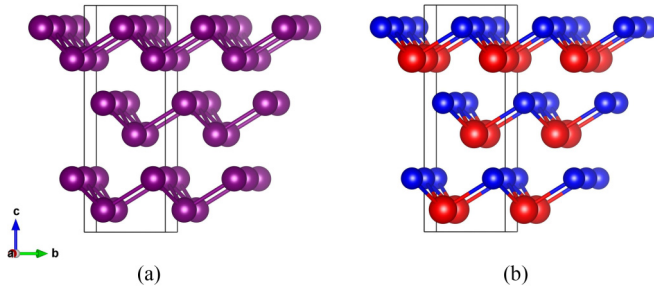


FIG. 1. (a) $A7$ -type structure of bismuth (Bi), antimony (Sb), and disordered solid solutions of $\text{Bi}_{1-x}\text{Sb}_x$. (b) A structurally ordered compound of bismuth antimonide (BiSb). The purple spheres in (a) represent either Bi or Sb atoms, while the red and blue spheres in (b) explicitly denote, respectively, Bi and Sb atoms. The thin black lines in both (a) and (b) outline the conventional hexagonal unit cells of the materials with each containing six atoms, representing three buckled sheets with a vertical stacking sequence of ABC .

atoms arrange themselves on a crystal lattice of the alloy under consideration. As a result, knowledge on the configurational thermodynamics of Bi and Sb is indeed crucially valuable information, as it provides a fundamental understanding on the alloying behavior of $\text{Bi}_{1-x}\text{Sb}_x$ under thermodynamic equilibrium conditions, and it can offer a possibility to probe an alloy design route for tuning and further enhancing the properties of $\text{Bi}_{1-x}\text{Sb}_x$ to fully enable utilization of the alloys in their future technological applications.

In this work, we use the first-principles cluster expansion in combination with the canonical Monte Carlo simulations to probe the alloying behavior of bulk/multilayer $\text{Bi}_{1-x}\text{Sb}_x$ at a given temperature T and alloy composition x . Since the robust SOC of Bi atoms has been reported in the literature to significantly affect the properties of Bi-containing compounds/alloys, including $\text{Bi}_{1-x}\text{Sb}_x$ [8,13–17], one would expect that it may, to a large extent, have an impact also on the phase stabilities of $\text{Bi}_{1-x}\text{Sb}_x$ solid solutions. Nevertheless, as far as we are aware, the influence of the SOC induced by Bi and probably Sb atoms on the alloying behavior of $\text{Bi}_{1-x}\text{Sb}_x$ has so far never been evaluated. Thus, in this work, the effect of SOC is also taken into account in deriving the configurational thermodynamics of Bi and Sb atoms to examine its consequence on the alloying behavior of $\text{Bi}_{1-x}\text{Sb}_x$. Interestingly, our results reveal that the SOC plays a crucial role in determining the configurational thermodynamics of Bi and Sb atoms, and thus the alloying behavior of $\text{Bi}_{1-x}\text{Sb}_x$. Without the effect of SOC, $\text{Bi}_{1-x}\text{Sb}_x$ displays chemical ordering of Bi and Sb atoms at low temperature to form an $A7$ -type ordered structure with the $R3m$ space group at $x = 0.5$, as illustrated by Fig. 1(b). Nevertheless, when the effect of SOC is taken into consideration, random solid solutions of $\text{Bi}_{1-x}\text{Sb}_x$ thermodynamically stable at elevated temperature is predicted to exhibit a tendency toward local segregation of Bi and Sb atoms at $T < 370$ K, and thus $\text{Bi}_{1-x}\text{Sb}_x$ is thermodynamically stable as a mixture of Bi-rich and Sb-rich $\text{Bi}_{1-x}\text{Sb}_x$ solid solutions without the formation of any ordered structure of $\text{Bi}_{1-x}\text{Sb}_x$, as predicted in the absence of SOC. A complete separation of the alloy constituents under thermodynamic equilibrium conditions, on the other hand, is predicted to achieve at

$T = 0$ K. These findings not only demonstrate that the SOC strongly affects the configurational thermodynamics of Bi and Sb atoms as well as the alloying behavior of $\text{Bi}_{1-x}\text{Sb}_x$, but also highlights an importance of considering the influence of SOC, when investigating the phase stabilities of alloys and compounds, composed of heavy elements.

II. METHODOLOGY

A. Cluster-expansion formalism

For a given atomic arrangement (σ) of Bi and Sb atoms on the $A7$ -type lattice, the mixing energy $\Delta E_{\text{mix}}(\sigma)$ of $\text{Bi}_{1-x}\text{Sb}_x$ solid solution with Bi and Sb contents given, respectively, by x_{Bi} and $x_{\text{Sb}} = 1 - x_{\text{Bi}}$, can be written as

$$\Delta E_{\text{mix}}(\sigma) = E(\sigma) - x_{\text{Bi}}E_{\text{Bi}} - x_{\text{Sb}}E_{\text{Sb}}, \quad (1)$$

where E_{Bi} and E_{Sb} stand, respectively, for the total energies of crystalline Bi and Sb, while the total energy of $\text{Bi}_{1-x}\text{Sb}_x$ of a given σ , denoted by $E(\sigma)$, can be formally expanded, according to the cluster-expansion (CE) formalism [31], into a sum over correlation functions $\xi_f^{(n)}(\sigma)$ of specific n -site figures f with the corresponding effective cluster interactions (ECIs) $V_f^{(n)}$:

$$E(\sigma) = \sum_f V_f^{(n)} \xi_f^{(n)}(\sigma). \quad (2)$$

Since the expression in Eq. (2) is mathematically complete only in the limit of inclusion of all possible f , it must be truncated for all practical purpose. Here, the MIT *ab initio* phase stability (MAPS) code [32], as implemented in the alloy-theoretic automated toolkit (ATAT) [33], is employed to truncate the expansion, expressed in Eq. (2), and to determine the ECIs in such a way that Eq. (2) returns $E(\sigma)$ of $\text{Bi}_{1-x}\text{Sb}_x$ as close to those obtained from first-principles calculations as possible for all σ , included in the expansion. The implementation of the cluster expansion to determine the ECIs and to derive the configurational thermodynamics of Bi and Sb atoms, constituting $\text{Bi}_{1-x}\text{Sb}_x$, will be provided and discussed in Secs. III A and III B, respectively.

B. First-principles calculations

The first-principles total energy of $\text{Bi}_{1-x}\text{Sb}_x$ solid solution is, for a given configuration σ , calculated from the density functional theory (DFT), in which the projector augmented wave (PAW) method [34] as implemented in the Vienna *ab initio* simulation package (VASP) [35,36] is used and the generalized gradient approximation [37] is employed to describe the exchange-correlation interactions. Here, the energy cutoff, included in the expansion of wave functions, is set to 500 eV, and the Monkhorst-Pack \mathbf{k} -point grid of $15 \times 15 \times 15$ are chosen for sampling the Brillouin zone [38]. The valence electron configurations, used for pseudopotentials, are $6s^2 6p^3$ and $5s^2 5p^3$ for Bi and Sb, respectively. To account for the weak interactions existing between the buckled sheets, the correction, proposed by Grimme (DFT-D3) [39], is added to the total-energy calculations. Moreover, in order to properly optimize the total energy of $\text{Bi}_{1-x}\text{Sb}_x$, the cell shape and volume of $\text{Bi}_{1-x}\text{Sb}_x$, including the internal atomic coordinates, are allowed to relax during the DFT calculations. Since, in

this work, we target at investigating the effect of SOC on the configurational thermodynamics of Bi and Sb atoms, two cases are hereby considered for deriving the total energy of $\text{Bi}_{1-x}\text{Sb}_x$ solid solutions, i.e., one with the effect of SOC and the other without the effect of SOC. In this work, the effect of SOC is evaluated by performing self-consistent-field cycles in the noncollinear mode. Note further that in VASP, the SOC is implemented by Kresse and Lebacqz [40], and the noncollinear calculations with the SOC is implemented by Hobbs *et al.* [41]. The electronic density of states of $\text{Bi}_{1-x}\text{Sb}_x$ is calculated using the tetrahedron method for the Brillouin zone integrations [42]. Note further that, for all DFT calculations, the total energies are ensured to converge within an accuracy of 1 meV/atom with respect both to the plane-wave energy cutoff and to the density of the \mathbf{k} -point grids.

C. Canonical Monte Carlo simulations

To investigate the alloying behavior of $\text{Bi}_{1-x}\text{Sb}_x$ solid solutions as a function of temperature and alloy composition in the absence and presence of the effect of SOC, we utilize the ECIs, obtained from the cluster expansion in each case, in canonical Monte Carlo (MC) simulations using the easy Monte Carlo code (EMC2) [43], as implemented in the ATAT [33]. In this work, the simulation boxes of $20 \times 20 \times 12$ rhombohedral primitive unit cells (9600 atoms) are employed to derive the configurational thermodynamics of Bi and Sb atoms. The simulations are performed at fixed compositions x , where $0 \leq x \leq 1$ and $\Delta x = 0.025$. At each composition, $\text{Bi}_{1-x}\text{Sb}_x$ solid solution is cooled from 3000 to 10 K with simulated annealing $\Delta T = 10$ K and at each temperature, the simulations include 18 000 MC steps for equilibrating the system and then 12 000 more steps for obtaining the proper averages of ΔE_{mix} and configurational specific heat C_V for $\text{Bi}_{1-x}\text{Sb}_x$ at different fixed temperatures and compositions. The alloying behavior of $\text{Bi}_{1-x}\text{Sb}_x$ solid solutions is then evaluated through the Gibbs free energy of mixing per atom ΔG_{mix} , given by

$$\Delta G_{\text{mix}}(x, T) = \Delta E_{\text{mix}}(x, T) - T \Delta S_{\text{mix}}(x, T), \quad (3)$$

where ΔS_{mix} denotes the mixing entropy per atom, and can be obtained from thermodynamic integration of C_V :

$$\Delta S_{\text{mix}}(x, T) = \Delta S_{\text{mix}}^{\text{MF}}(x) + \int_{\infty}^T \frac{C_V(x, T')}{T'} dT'. \quad (4)$$

The term $\Delta S_{\text{mix}}^{\text{MF}}$ is, on the other hand, described as the mixing entropy per atom of the ideally random solid solution of the alloy, stable in the limit of $T \rightarrow \infty$, and it can thus be derived from the mean-field approach to be

$$\Delta S_{\text{mix}}^{\text{MF}}(x) = -k_B [x \ln(x) + (1-x) \ln(1-x)]. \quad (5)$$

For this particular case, we assume that $\Delta S_{\text{mix}}(x, T = 3000 \text{ K}) \approx \Delta S_{\text{mix}}^{\text{MF}}(x)$, and thus the thermodynamic integration in Eq. (4) is performed from this high temperature downward to the temperature of interest.

III. RESULTS AND DISCUSSION

A. Cluster expansions of $\text{Bi}_{1-x}\text{Sb}_x$ solid solutions

To investigate the alloying behavior of $\text{Bi}_{1-x}\text{Sb}_x$, we as a first step use an algorithm [44] to establish a set of 3502 σ of Bi and Sb atoms based on the A7-type lattice up to 12 atoms in the primitive supercell, equivalent to 6 primitive rhombohedral unit cells. From this set, around 100 σ are singled out starting with small unit cell σ , and we employ the first-principles approach to calculate the total energy of those selected σ , which are subsequently served as input for the cluster expansion to derive ECIs. The initial set of ECIs is then utilized to predict the total energy of all generated σ using Eq. (2), although it may not do the prediction accurately. Consequently, to further improve the predictive power of the ECIs, we do as follows: (1) reestablish a set of input σ focusing particularly on low energy σ of $\text{Bi}_{1-x}\text{Sb}_x$, guided by the initial set of ECIs, (2) perform the first-principles calculations to compute their total energy, and (3) perform the cluster expansion by using the new set of input σ , as established in (1), to determine the ECIs. This procedure can be repeated in an iterative manner, until the ECIs of desired quality are obtained for the both cases of $\text{Bi}_{1-x}\text{Sb}_x$ under consideration, i.e., with and without the effect of SOC.

Since we have to truncate the expression in Eq. (2) to a finite number of terms for all practical purposes, as stated in Sec. II A, it is not feasible to determine the exact cluster expansion and to precisely know the ECIs for all possible figures f , which are theoretically infinite. Then, a question arises concerning how many terms in the expansion should be retained without losing the expansion's predictive power, given that the first-principles total energies of a certain number of input σ are known. If too few terms are kept, the derived ECIs may not be able to account for all sources of energy fluctuations, generally leading to poor predictions of the total energies and thus a large value of the mean-squared error of the predicted energies. On the other hand, the mean-squared error may appear small, if too many terms are kept in the expansion. However, in such a case, the derived ECIs tend to overfit the total energies of those served as input σ for the cluster expansion, while their predictive power for σ , which is not included in the expansion, can be severely low. In practice, one can find an optimal number of terms to be kept as well as the choice of ECIs representing the best compromise between the two cases, mentioned above, by evaluating the predictive power of the expansion using the cross-validation score. Further details regarding the procedure to truncate the expansion, as implemented in the MAPS code, as well as the cross-validation score can be found elsewhere [32].

In the case of the absence (presence) of the influence of SOC induced by Bi and Sb atoms, the final expansion includes 191 (187) σ and utilizes a total of 35 (33) ECIs. That is, apart from the zero-site and one-site interactions, the ECIs obtained from the final expansion with (without) the impact of SOC are composed of 19 (21) two-site and 12 (12) three-site interactions, and thus the final expansion fits the energies of the 187 (191) input σ with the cross-validation score of 0.778 (0.363) meV/atom indicating the predictive power of the derived ECIs. Figures 2(a) and 2(b) illustrate ΔE_{mix} at $T = 0$ K of all generated σ of $\text{Bi}_{1-x}\text{Sb}_x$, determined with

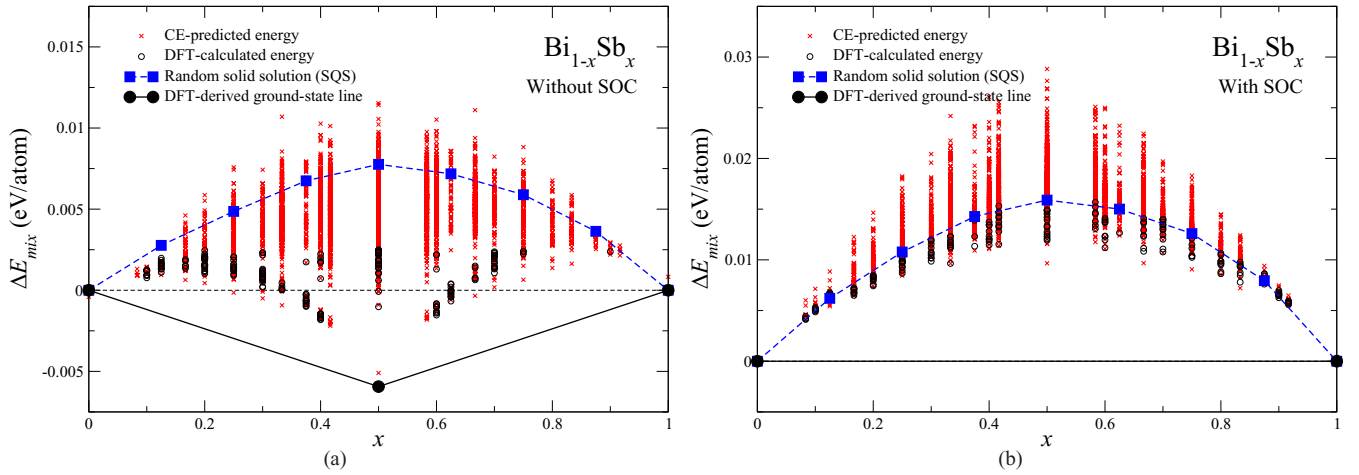


FIG. 2. Ground-state diagram at $T = 0$ K of multilayer $\text{Bi}_{1-x}\text{Sb}_x$ with (a) the absence of the effect of SOC and (b) the presence of the effect of SOC. Red crosses are the CE-predicted energies of mixing ΔE_{mix} of all generated σ . Open black circles are the DFT-calculated ΔE_{mix} of the selected σ , included in the final cluster expansions. Thick black lines, connecting two large filled black circles both in (a) and in (b), represent the DFT-derived ground-state lines of $\text{Bi}_{1-x}\text{Sb}_x$, while filled blue squares stand for the DFT-calculated ΔE_{mix} of the completely random solid solutions of $\text{Bi}_{1-x}\text{Sb}_x$ modeled by the SQS method.

respect to Bi and Sb, in the absence and presence of the effect of SOC, respectively. Also, we give in Fig. 2 DFT-calculated ΔE_{mix} of ideally random $\text{Bi}_{1-x}\text{Sb}_x$ solid solutions for comparison to the results derived from the cluster expansion. In this case, the completely random solid solutions of $\text{Bi}_{1-x}\text{Sb}_x$ are modeled within 64-atom supercells, where $0 \leq x \leq 1$ and $\Delta x = 0.125$, by employing the special quasirandom structure (SQS) method [45].

First, we consider the case of which the influence of SOC is neglected, as displayed by Fig. 2(a). In this case, our results reveal that, aside from the elemental phases of the constituent atoms, i.e., Bi and Sb, $\text{Bi}_{1-x}\text{Sb}_x$ display chemical ordering of Bi and Sb atoms, thus leading to a formation of a stable compound at $x = 0.5$ [see Fig. 1(b) for visualization of its atomic arrangement], as indicated by the DFT-derived ground-state line in Fig. 2(a). Such an ordered compound of BiSb is found to exhibit exactly the same atomic configuration as that of $\text{As}_{1-x}\text{Sb}_x$ at $x = 0.5$, recently observed in experiment [29] and reported to be thermodynamically stable upon annealing up to $T \approx 475$ K [30]. These results further suggest that, at $T = 0$ K, $\text{Bi}_{1-x}\text{Sb}_x$ solid solution, where $x < 0.5$ ($x > 0.5$), will decompose into and thus be stable as a mixture of the ordered compound of BiSb and the elemental phase of Bi (Sb). Nevertheless, we find that whenever the effect of SOC is taken into account, ΔE_{mix} of $\text{Bi}_{1-x}\text{Sb}_x$ solid solution becomes positive for all considered σ , including those modeled by the SQS approach [see Fig. 2(b)]. This indicates that in the presence of the influence of SOC and at $T = 0$ K, $\text{Bi}_{1-x}\text{Sb}_x$ exhibit, instead of chemical ordering of Bi and Sb atoms, chemical clustering of Bi and Sb atoms, i.e., phase separation of the constituents, across the entire composition range in thermodynamic equilibrium. The remarkable difference in the phase stability at $T = 0$ K of $\text{Bi}_{1-x}\text{Sb}_x$ between the absence and presence of the effect of SOC, as can be seen from Fig. 2, explicitly implies that the SOC plays a crucial role in determining the configurational thermodynamics of Bi and Sb atoms, which in turn governs the alloying behavior of $\text{Bi}_{1-x}\text{Sb}_x$ solid solutions. In the following section, detailed

discussion on the alloying behavior of $\text{Bi}_{1-x}\text{Sb}_x$ as a function of temperature and alloy composition in the presence of the effect of SOC will be provided.

It should also be noted that the thermodynamic stability at $T = 0$ K of the ordered structure of $\text{Bi}_{1-x}\text{Sb}_x$ at $x = 0.5$, as shown in Fig. 1(b), was theoretically considered and previously reported by Singh *et al.* [13]. Their results suggested that, in spite of the presence of the effect of SOC, the said ordered structure is thermodynamically stable with respect to Bi and Sb, whose ΔE_{mix} is -14.90 meV/atom. This is in contrast to the results, calculated in this work. With the inclusion of the effect of SOC, our results reveal that ΔE_{mix} of the ordered structure shown in Fig. 1(b) is $+17.54$ meV/atom, which is even higher than that of the completely random solid solution of $\text{Bi}_{1-x}\text{Sb}_x$ at $x = 0.5$ ($+15.89$ meV/atom) by 1.65 meV/atom. Before identifying the source of such discrepancy in ΔE_{mix} of the ordered compound of BiSb, it is worth mentioning that the first-principles total energies of $\text{Bi}_{1-x}\text{Sb}_x$ alloys and their competing phases (Bi and Sb), reported in Ref. [13], were essentially derived from the same methodological approaches used in this work. Those are, the PAW method [34] plus the inclusion of the SOC, as implemented in the VASP code [35,36,40,41], and the generalized gradient approximation for modeling the exchange-correlation effects [37]. Apart from the input values for the energy cutoff and the density of the Monkhorst-Pack \mathbf{k} -point grids, the main differences in determining ΔE_{mix} of $\text{Bi}_{1-x}\text{Sb}_x$ between our work and that of Singh *et al.* [13] can be assigned as follows: first, the correction to the total energy due to the weak interactions existing between the buckled sheet of $\text{Bi}_{1-x}\text{Sb}_x$ [39] was not included in the total-energy calculations of Singh *et al.* [13] and second, the valence electron configuration for the pseudopotential of Bi, used in Singh *et al.* [13], was $5d^{10}6s^26p^3$, while in our case it is $6s^26p^3$. However, we find through our investigation that the inclusion of the 10 $5d$ electrons as valence electrons for the pseudopotential of Bi and the absence of the weak interactions coupling between the buckled sheets both do have a minimal

TABLE I. First-principles total energy per atom (E_{tot}) of Bi, Sb, the ordered compound of BiSb, shown in Fig. 1(a) and the ideally random solid solution of $\text{Bi}_{1-x}\text{Sb}_x$ at $x = 0.5$, modeled by the SQS method, evaluated in this work with and without the inclusion of the influence of SOC.

	E_{tot} (eV/atom)	
	Without SOC	With SOC
Bi	-4.175	-4.747
BiSb		
Ordered compound	-4.290	-4.587
Ideally random solid solution	-4.277	-4.589
Sb	-4.393	-4.461

impact on ΔE_{mix} of $\text{Bi}_{1-x}\text{Sb}_x$, where the change in ΔE_{mix} of the ordered compound of BiSb due to the two said points is less than 1 meV/atom. However, we notice that if we use the total energy of Sb, evaluated without the inclusion of the effect of SOC, to determine ΔE_{mix} of the ordered compound of BiSb with the influence of SOC taken into account in deriving the total energy both of BiSb and of Bi, ΔE_{mix} of BiSb under consideration decreases from +17.54 to -16.06 meV/atom, very close to the value of -14.90 meV/atom reported by Singh *et al.* [13]. To further verify whether the difference in ΔE_{mix} of $\text{Bi}_{1-x}\text{Sb}_x$ between this work and that of Singh *et al.* [13] is actually a result from the absence of SOC in Sb, we consider ΔE_{mix} of the ordered structure of $\text{Bi}_{1-x}\text{Sb}_x$ at $x = 0.25$ or Bi_3Sb , composed of alternating layers of Bi and BiSb in a superlattice with the $R3m$ space group [see Fig. 10(a) in Ref. [13]]. Singh *et al.* [13] reported a value of -6.3 meV/atom for ΔE_{mix} of such an ordered Bi_3Sb , while for this particular σ our calculations yield ΔE_{mix} of +12.74 meV/atom. If the effect of SOC is neglected only for Sb, we find that ΔE_{mix} of Bi_3Sb under consideration changes from +12.74 to -4.23 meV/atom, again similar to the value reported in Ref. [13]. As shown by these results, we thus propose that the source of the aforementioned discrepancy in ΔE_{mix} of $\text{Bi}_{1-x}\text{Sb}_x$ may be due to the lack of SOC when evaluating the total energy of Sb, and also put in question the thermodynamic stability of different structures of $\text{Bi}_{1-x}\text{Sb}_x$ in Ref. [13]. Furthermore, in the following section, the evidence showing the reliability of our used theoretical approach will be additionally provided.

For further comparison with the earlier works reported, for example, by Singh *et al.* [13] and also the future theoretical works on $\text{Bi}_{1-x}\text{Sb}_x$, we list in Table I values of first-principles total energy per atom of Bi, Sb, and BiSb [both the ordered compound, illustrated by Fig. 1(b) and the ideally random solid solution, modeled by the SQS method], calculated in this work without and with the inclusion of the influence of SOC.

B. Alloying behavior of $\text{Bi}_{1-x}\text{Sb}_x$ solid solutions

As briefly mentioned in Sec. III A, the configurational thermodynamics of Bi and Sb atoms is, to a large degree, sensitive to the effect of SOC, and we have demonstrated that for $\text{Bi}_{1-x}\text{Sb}_x$ the SOC results in the disappearance of chemical ordering of the constituent elements, as can be seen from

Fig. 2(b). Furthermore, since the SOC is indeed an intrinsic material property, the scenario of which $\text{Bi}_{1-x}\text{Sb}_x$ displays chemical ordering of Bi and Sb at $x = 0.5$, as depicted in Fig. 2(a), may in reality never exist, and to the best of our knowledge, no observation of such an ordered $\text{Bi}_{1-x}\text{Sb}_x$ at $x = 0.5$ has ever been reported in the literature. For this reason, the configurational thermodynamics of Bi and Sb only in the presence of the effect of SOC will be considered in the present section. To do so, we utilize the ECIs obtained from the final expansion in the canonical MC simulations, as described in Sec. II C, to evaluate ΔG_{mix} as a function of temperature and alloy composition. In Sec. III A, we have demonstrated that, as $T \rightarrow 0$ K, $\text{Bi}_{1-x}\text{Sb}_x$ exhibit chemical clustering of Bi and Sb atoms, i.e., phase separation of the constituents. This typically results in a boundary line separating a single-phase region and a two-phase region (a miscibility gap) in a phase diagram. However, it must be emphasized that the thermodynamic integration path using Eq. (4) across such a boundary between the two regions is impossible. This is because, at the conditions of phase separation of the alloy constituents, the canonical MC-derived C_V shows a tremendous value and is not a continuous function, which numerically makes the integration results, i.e., ΔS_{mix} , undefined. As a consequence, the thermodynamic integrations and thus evaluation of ΔG_{mix} for this particular case will be valid, only when the integrations are performed from high temperature, where $\text{Bi}_{1-x}\text{Sb}_x$ is stable as a single-phase solid solution, downward to the temperature at which the phase separation of the alloy constituents takes place.

Figure 3(a) displays ΔG_{mix} curves of $\text{Bi}_{1-x}\text{Sb}_x$ at some selected temperatures, in which the effect of SOC is taken into account. We find that ΔG_{mix} of $\text{Bi}_{1-x}\text{Sb}_x$ in the presence of SOC exhibits a positive curvature for the whole composition range already at $T \approx 380$ K and above, indicating formation of a continuous series of single-phase solid solutions of $\text{Bi}_{1-x}\text{Sb}_x$. By applying the common-tangent construction to ΔG_{mix} at different fixed temperatures, we sketch a phase diagram of $\text{Bi}_{1-x}\text{Sb}_x$ in the presence of SOC [see Fig. 3(b)]. The phase diagram reveals that a complete closure of a miscibility gap takes place at $T \approx 370$ K. At $T > 370$ K, $\text{Bi}_{1-x}\text{Sb}_x$ is thermodynamically stable as a single-phase solid solution (α) over the entire composition range. At $T \lesssim 370$ K, $\text{Bi}_{1-x}\text{Sb}_x$ is predicted to exhibit a tendency toward local segregation of Bi and Sb, and as a result $\text{Bi}_{1-x}\text{Sb}_x$ is stable in thermodynamic equilibrium as a mixture of Bi-rich and Sb-rich $\text{Bi}_{1-x}\text{Sb}_x$ solid solutions, i.e., α' and α'' , respectively. It is worth pointing out that the isostructural phase diagram of $\text{Bi}_{1-x}\text{Sb}_x$, shown in Fig. 3(b), is in good agreement with the low-temperature part of the phase diagram of the binary Bi-Sb system, recently obtained by the calculation of phase diagrams (CALPHAD) assessment of experimental thermodynamics [28]. Moreover, the critical temperature at which the miscibility gap appears, as predicted in this work, is nearly identical to that, reported in Ref. [28]. Note further that, although a complete separation of the constituent elements under the thermodynamic equilibrium conditions is presumed to achieve at $T = 0$ K as indicated by positive ΔE_{mix} at all compositions x [see Fig. 2(b)], our results show that, in the presence of the SOC, Bi and Sb readily mix with each other to form a random solid solution of $\text{Bi}_{1-x}\text{Sb}_x$, as the temperature increases. This is attributed not only to the increasingly influential contribution

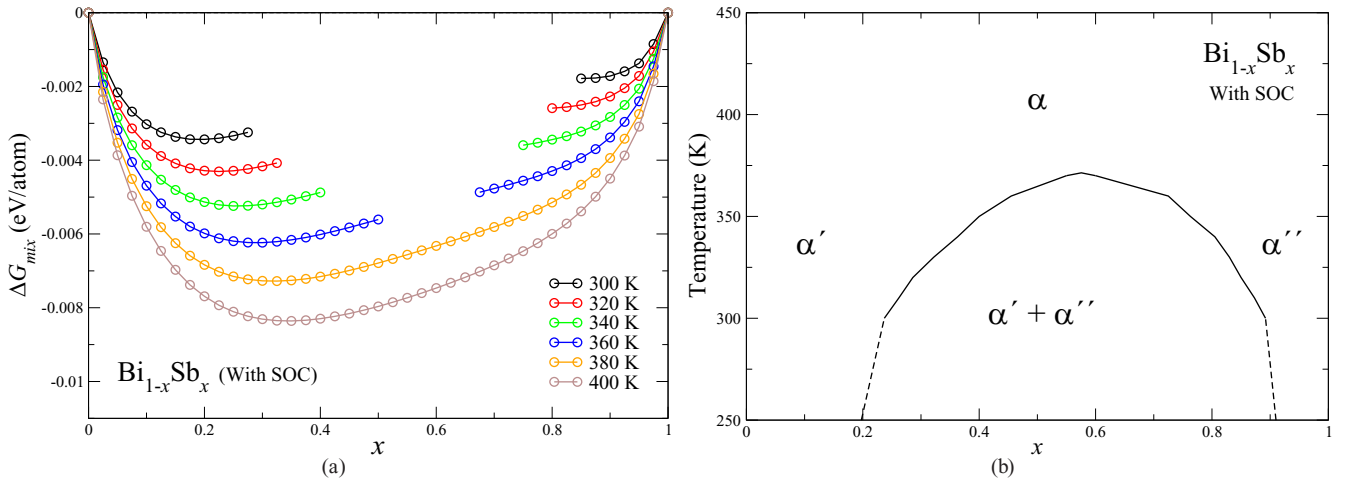


FIG. 3. (a) ΔG_{mix} of $\text{Bi}_{1-x}\text{Sb}_x$ at $T = 300, 320, 340, 360, 380,$ and 400 K, evaluated by taking into account the effect of SOC. (b) Isostructural phase diagram of $\text{Bi}_{1-x}\text{Sb}_x$ in the presence of the effect of SOC (see the main text for description).

of ΔS_{mix} to ΔG_{mix} , but also to relatively weak ECIs in the binary Bi-Sb system. The latter gives rise to the driving force to form a random solid solution of $\text{Bi}_{1-x}\text{Sb}_x$, stable in the limit $V/T \rightarrow 0$, where V is defined as the strongest interaction in the Bi-Sb system [46]. Here, we find that, under the influence of SOC, the magnitude of the ECIs, derived from the final cluster expansion of $\text{Bi}_{1-x}\text{Sb}_x$ is smaller than ~ 2.5 meV/atom, as illustrated by Fig. 4(a), and consequently the criterion $V/T \rightarrow 0$, characterizing the feature of random solid solutions, can be fulfilled at elevated temperature. In order to verify that, at elevated temperature, $\text{Bi}_{1-x}\text{Sb}_x$ typically behaves like a random solid solution, we evaluate ΔG_{mix} of an ideally random solid solution of $\text{Bi}_{1-x}\text{Sb}_x$, modeled with the SQS method, and then for a given temperature compare it to that evaluated from the MC simulations, as can be seen from Fig. 4(b). Since in this work the mixing energies ΔE_{mix} of the ideally random solid solutions of $\text{Bi}_{1-x}\text{Sb}_x$ are evaluated at discrete grids with $x = 0, 0.125, 0.25, 0.375, 0.5,$

$0.625, 0.75, 0.875,$ and 1 , they are fitted *via* a cubic spline interpolation and then combined with $-T\Delta S_{\text{mix}}$, where ΔS_{mix} was analytically evaluated by using the mean-field approach, as expressed by Eq. (5), with Δx of 0.025 to obtain ΔG_{mix} of the ideally random solid solutions of $\text{Bi}_{1-x}\text{Sb}_x$. We find that ΔG_{mix} of $\text{Bi}_{1-x}\text{Sb}_x$, estimated *via* the mean-field approach, is very close to that derived from the MC simulations even at room temperature ($T \approx 300$ K). Quantitatively, the difference in ΔG_{mix} between the two approaches, shown in Fig. 4(b), is found to be less than 1 meV/atom, thus indicating that at $\text{Bi}_{1-x}\text{Sb}_x$ behaves like a random solid solution already at $T \gtrsim 300$ K.

It is worth noting that, in this work, the contributions, originating from the lattice vibrations or the phonons, to ΔG_{mix} of $\text{Bi}_{1-x}\text{Sb}_x$ is being neglected. This is because, for isostructural alloys, such contributions are typically of minor importance in comparison with the contributions arising from the configurational disorder of the alloy constituents on the

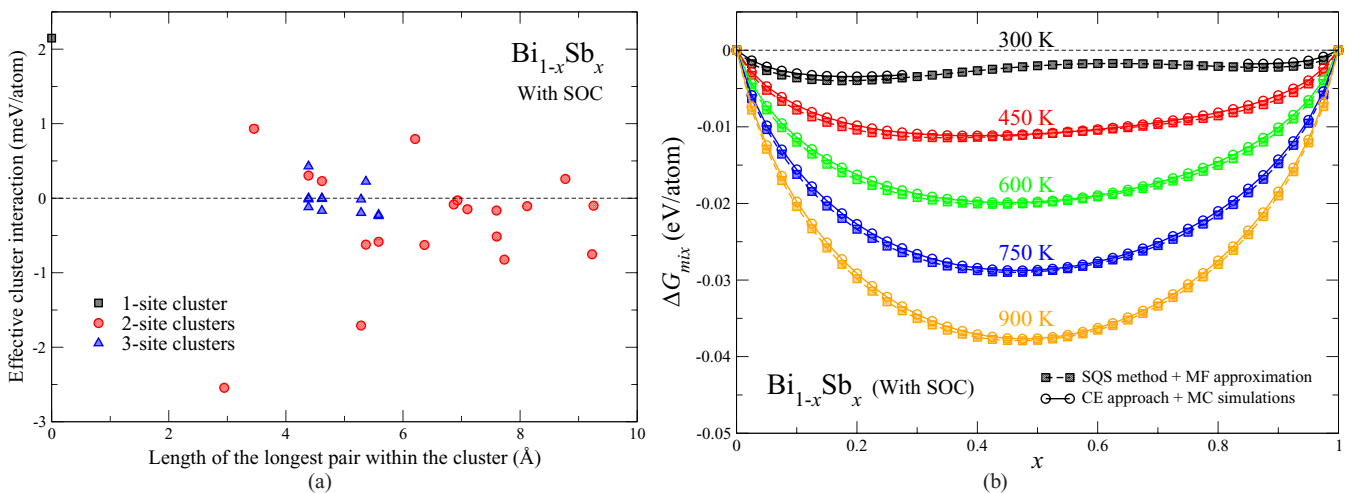


FIG. 4. (a) Strength of effective cluster interactions (ECIs), obtained from the final expansion including the 187 input σ of $\text{Bi}_{1-x}\text{Sb}_x$ in the presence of the effect of SOC. (b) ΔG_{mix} of $\text{Bi}_{1-x}\text{Sb}_x$ at $T = 300, 450, 600, 750,$ and 900 K under the influence of SOC, as obtained from canonical MC simulations (open circles) and mean-field (MF) approximation (shaded squares).

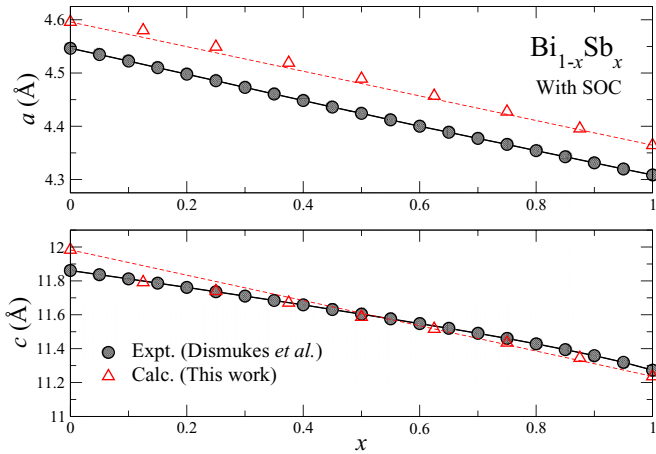


FIG. 5. a and c lattice parameter of random solid solutions of $\text{Bi}_{1-x}\text{Sb}_x$ as a function of composition x , calculated in this work (red triangles). The red dashed lines indicate the lattice parameters calculated according to the Vegard's law between Bi and Sb. Comparison is made with the experimental data, previously reported by Dismukes *et al.* [19] (shaded black circles).

lattice sites. In addition, we found in our previous works [47,48] that, for a given alloy composition, the degree of configurational disorder of alloy constituents has a minimal impact on the phonon density of states and thus the vibrational free energy, if the structural properties, for example, lattice parameters, bond lengths, and bond angles, of the disordered alloys do not, on average, significantly differ from those of the ordered ones. In this work, the lattice parameters predicted for ordered $\text{Bi}_{1-x}\text{Sb}_x$ are different from those of disordered solid solutions of $\text{Bi}_{1-x}\text{Sb}_x$, considered at the same composition, by less than 0.5%, whether or not the effect of SOC is present. These results indicate that, for the Bi-Sb system, both the degree of configurational disorder of Bi and Sb atoms and the SOC are likely to have a tiny effect on the mixing vibrational free energy of $\text{Bi}_{1-x}\text{Sb}_x$ solid solutions at a given alloy composition. Considering this, together with our findings that in the presence of SOC $\text{Bi}_{1-x}\text{Sb}_x$ is thermodynamically stable as a single-phase solid solution across the entire composition range at $T > 370$ K, the influence of phonons for this particular case should be very small at such a relatively low temperature and thus likely does not yield a significant impact on the alloying behavior of $\text{Bi}_{1-x}\text{Sb}_x$, predicted in this work and shown in Fig. 3(b).

Besides, we find that the lattice parameters of random solid solutions of $\text{Bi}_{1-x}\text{Sb}_x$, calculated in this work, are in good agreement with the experiments [19]. Here, our theoretical values do differ from the experimental ones by less than 1.5%, and they only slightly deviate from the values calculated according to the Vegard's law between Bi and Sb by less than 0.3%, as shown in Fig. 5. Furthermore, it has been experimentally demonstrated [49–51] that the $\text{Bi}_{1-x}\text{Sb}_x$ solid solution can behave as a small-band-gap semiconductor within a narrow composition range of which $0.07 < x < 0.22$, while for $x \lesssim 0.07$ and $x \gtrsim 0.22$, it is semimetallic. The origin of the semiconducting properties of $\text{Bi}_{1-x}\text{Sb}_x$ with $0.07 < x < 0.22$ can be interpreted by the disappearance of the overlap between the valence band maximum at the T

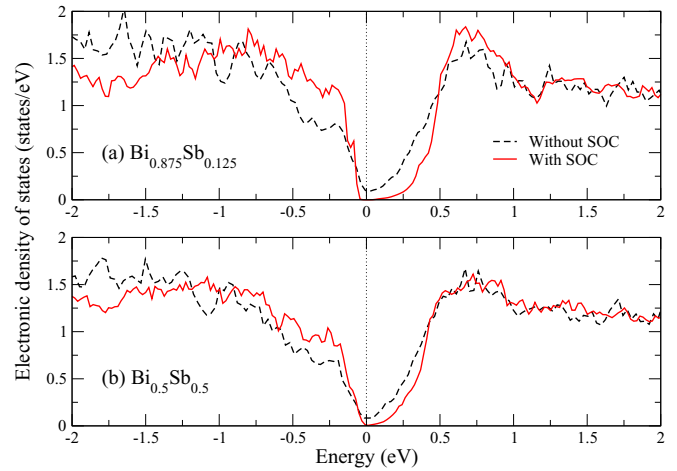


FIG. 6. Electronic density of states around the highest occupied state, indicated by the vertical dotted lines at 0 eV, of (a) $\text{Bi}_{0.875}\text{Sb}_{0.125}$ and (b) $\text{Bi}_{0.5}\text{Sb}_{0.5}$ disordered solid solutions.

point and the conduction band minimum at the L point of the first Brillouin zone, and also the inversion of the two L bands [49–51]. By inspecting the electronic density of states of the disordered solid solutions of $\text{Bi}_{1-x}\text{Sb}_x$, modeled by the SQS technique, we observe that in the absence of the effect of SOC $\text{Bi}_{1-x}\text{Sb}_x$ is semimetallic for all considered compositions, where $0 \leq x \leq 1$ and $\Delta x = 0.125$. We, however, find that a small band gap of ~ 30 meV is predicted for $\text{Bi}_{1-x}\text{Sb}_x$ at $x = 0.125$, only if the effect of SOC is taken into account in deriving the density of states, as shown in Fig. 6(a). The disordered solid solution of $\text{Bi}_{1-x}\text{Sb}_x$ with $x = 0.5$ is, on the other hand, predicted to be a semimetal irrespective of the presence of SOC [see Fig. 6(b)]. These results suggest that, to reach an accurate qualitative description on the electronic behavior of the disordered solid solutions of $\text{Bi}_{1-x}\text{Sb}_x$, which is in line with the experimental observations [49–51], the effect of SOC must be considered. A fairly good agreement both in the lattice parameters and in the electronic density of states of disordered $\text{Bi}_{1-x}\text{Sb}_x$ solid solutions between our theoretical calculations, where the effect of SOC is taken into consideration, and the experimental observations, previously reported in the literature, not only emphasizes an essential role of the SOC in determining the properties of $\text{Bi}_{1-x}\text{Sb}_x$, but also provides additional evidence strengthening the reliability of our methodological approach used in this work.

Our prediction on the alloying behavior of $\text{Bi}_{1-x}\text{Sb}_x$ is, in fact, in line with the experimental phase diagrams of the binary Bi-Sb system, previously proposed in the literature [27,28] and revealing that thermodynamically Bi and Sb atoms form a continuous series of disordered solid solutions over the whole composition range at $T \gtrsim 450$ K. In practice, solid solutions of $\text{Bi}_{1-x}\text{Sb}_x$ [α in Fig. 3(b)] are generally prepared from molten mixture of Bi and Sb by using the zone-leveling technique [1,2]. Even though our phase diagram, Fig. 2(b), suggests that $\text{Bi}_{1-x}\text{Sb}_x$ in equilibrium can exhibit a tendency toward local phase segregation into Bi and Sb (α' and α'') as $T \rightarrow 0$ K, one can expect that upon cooling the melt to, for example, room temperature α is likely to persist, while clustering of Bi and Sb seems unlikely due to slow

diffusion of the constituent elements at low temperature ($T < 450$ K). In spite of the disappearance of chemical ordering of Bi and Sb due to the effect of SOC, it is still feasible to employ low-temperature synthesis techniques, where the atomic diffusion/mobility is kinetically limited (for example, molecular beam epitaxy) to fabricate metastable ordered structures of $\text{Bi}_{1-x}\text{Sb}_x$, composed of alternating thin layers of Bi and Sb in a superlattice [52]. Utilizing such techniques indirectly offers an opportunity to tailor and further improve the thermoelectric electric figure of merit of $\text{Bi}_{1-x}\text{Sb}_x$ since it has also been shown that the properties of the said Bi/Sb superlattice alloys, such as, electronic band structure, thermal conductivity, and Seebeck coefficient, are dependent on the thickness of the Bi and Sb layers [52].

IV. CONCLUSION

The role of spin-orbit coupling in the alloying behavior of multilayer $\text{Bi}_{1-x}\text{Sb}_x$ solid solutions is studied using a first-principles cluster-expansion method in combination with canonical Monte Carlo simulations. We reveal that, without the effect of spin-orbit coupling, $\text{Bi}_{1-x}\text{Sb}_x$ displays chemical ordering of Bi and Sb atoms, giving rise to formation of an ordered structure of $\text{Bi}_{1-x}\text{Sb}_x$ at $x \approx 0.5$ at low temperature. Nevertheless, owing to robust spin-orbit coupling effect intrinsically induced by heavy Bi and Sb atoms, $\text{Bi}_{1-x}\text{Sb}_x$ thermodynamically stable as a single-phase random solid solution at $T \gtrsim 370$ K exhibits instead a clustering tendency toward

local segregation of Bi and Sb atoms at low temperature, i.e., at $T < 370$ K, and thus two solid solutions of $\text{Bi}_{1-x}\text{Sb}_x$ of different compositions x , i.e., Bi-rich and Sb-rich $\text{Bi}_{1-x}\text{Sb}_x$, coexist in thermodynamic equilibrium without formation of any ordered structure of $\text{Bi}_{1-x}\text{Sb}_x$ as predicted in the absence of the effect of spin-orbit coupling. Evidently, these findings not only demonstrate the strong effect of spin-orbit coupling on the alloying behavior of $\text{Bi}_{1-x}\text{Sb}_x$, but also highlight an importance of considering the influence of spin-orbit coupling, when investigating the phase stabilities of alloys/compounds composed of heavy elements.

ACKNOWLEDGMENTS

This research is funded by Chulalongkorn University: CU-GR_62_66_23_26. A.E. gratefully acknowledges the support from the Thailand Toray Science Foundation (TTSF). B.A. acknowledges financial support from the Swedish Government Strategic Research Area in Materials Science on Functional Materials at Linköping University, Faculty Grant SFOMatLiU No. 2009 00971, as well as support from the Swedish Foundation for Strategic Research through the Future Research Leaders 6 program, FFL 15-0290, from the Swedish Research Council (VR) through the Grant No. 2019-05403, and Knut and Alice Wallenberg Foundation (Wallenberg Scholar Grant No. KAW-2018.0194). All calculations are carried out using supercomputer resources provided by the Swedish National Infrastructure for Computing (SNIC) performed at the National Supercomputer Centre (NSC).

-
- [1] G. E. Smith and R. Wolfe, Thermoelectric properties of bismuth-antimony alloys, *J. Appl. Phys.* **33**, 841 (1962).
- [2] H. J. Goldsmid, Bismuth-antimony alloys, *Phys. Status Solidi A* **1**, 7 (1970).
- [3] A. M. Ibrahim and D. A. Thompson, Thermoelectric properties of BiSb alloys, *Mater. Chem. Phys.* **12**, 29 (1985).
- [4] B. Lenoir, M. Cassart, J.-P. Michenaud, H. Scherrer, and S. Scherrer, Transport properties of Bi-RICH Bi-Sb alloys, *J. Phys. Chem. Solids* **57**, 89 (1996).
- [5] V. S. Zemskov, A. D. Belaya, U. S. Beluy, and G. N. Kozhemyakin, Growth and investigation of thermoelectric properties of Bi-Sb alloy single crystals, *J. Cryst. Growth* **212**, 161 (2000).
- [6] Y.-M. Lin, O. Rabin, S. B. Cronin, J. Y. Ying, and M. S. Dresselhaus, Semimetal-semiconductor transition in $\text{Bi}_{1-x}\text{Sb}_x$ alloy nanowires and their thermoelectric properties, *Appl. Phys. Lett.* **81**, 2403 (2002).
- [7] J. C. Y. Teo, L. Fu, and C. L. Kane, Surface states and topological invariants in three-dimensional topological insulators: Application to $\text{Bi}_{1-x}\text{Sb}_x$, *Phys. Rev. B* **78**, 045426 (2008).
- [8] H.-J. Zhang, C.-X. Liu, X.-L. Qi, X.-Y. Deng, X. Dai, S.-C. Zhang, and Z. Fang, Electronic structures and surface states of the topological insulator $\text{Bi}_{1-x}\text{Sb}_x$, *Phys. Rev. B* **80**, 085307 (2009).
- [9] H. Y. Lv, H. J. Liu, L. Pan, Y. W. Wen, X. J. Tan, J. Shi, and X. F. Tang, Structural, electronic, and thermoelectric properties of BiSb nanotubes, *J. Phys. Chem. C* **114**, 21234 (2010).
- [10] S. Lee, K. Esfarjani, J. Mendoza, M. S. Dresselhaus, and G. Chen, Lattice thermal conductivity of Bi, Sb, and Bi-Sb alloy from first principles, *Phys. Rev. B* **89**, 085206 (2014).
- [11] E. Güneş, B. Landschreiber, D. Hartung, M. T. Elm, C. Rohner, P. J. Klar, and S. Schlecht, Effect of bismuth nanotubes on the thermoelectric properties of BiSb alloy nanocomposites, *J. Electron Mater.* **43**, 2127 (2014).
- [12] Z. Zhu, J. Guan, and D. Tománek, Structural transition in layered $\text{As}_{1-x}\text{P}_x$ compounds: A computational study, *Nano Lett.* **15**, 6042 (2015).
- [13] S. Singh, W. Ibarra-Hernández, I. Valencia-Jaime, G. Avendaño-Franco, and A. H. Romero, Investigation of novel crystal structures of Bi-Sb binaries predicted using the minima hopping method, *Phys. Chem. Chem. Phys.* **18**, 29771 (2016).
- [14] S. Singh, A. C. Gracia-Castro, I. Valencia-Jaime, F. Muñoz, and A. H. Romero, Prediction and control of spin polarization in a Weyl semimetallic phase of BiSb, *Phys. Rev. B* **94**, 161116(R) (2016).
- [15] S. Singh and A. H. Romero, Giant tunable Rashba spin splitting in a two-dimensional BiSb monolayer and in BiSb/AlN heterostructures, *Phys. Rev. B* **95**, 165444 (2017).
- [16] J. Yuan, Y. Cai, L. Shen, Y. Xiao, J.-C. Ren, A. Wang, Y. P. Feng, and X. Yan, One-dimensional thermoelectrics induced by Rashba spin-orbit coupling in two-dimensional BiSb monolayer, *Nano Energy* **52**, 163 (2018).
- [17] S. Singh, I. Valencia-Jaime, O. Pavlic, and A. H. Romero, Elastic, mechanical, and thermodynamic properties of

- Bi-Sb binaries: Effect of spin-orbit coupling, *Phys. Rev. B* **97**, 054108 (2018).
- [18] D. T. Do, Electronic structure and thermoelectric properties of monolayer of group V atoms, in *Advanced Materials: Proceedings of the International Workshop on Advanced Materials (IWAM-2017)*, AIP Conference Proceedings, Vol. 2005 (AIP Publishing, Melville, NY, 2018), p. 020005.
- [19] J. P. Dismukes, R. J. Paff, R. T. Smith, and R. Ulmer, Lattice parameter and density in bismuth-antimony alloys, *J. Chem. Eng. Data* **13**, 317 (1968).
- [20] P. Ares, F. Aguilar-Galindo, D. Rodriguez-San-Miguel, D. A. Aldave, S. Diaz-Tendero, M. Alcami, F. Martin, J. Gomez-Herrero, and F. Zamora, Mechanical isolation of highly stable antimonene under ambient conditions, *Adv. Mater.* **28**, 6332 (2016).
- [21] R. Gusmão, Z. Sofer, D. Bouša, and M. Pumera, Pnictogen (As, Sb, Bi) nanosheets for electrochemical applications are produced by shear exfoliation using kitchen blenders, *Angew. Chem. Int. Ed.* **56**, 14417 (2017).
- [22] J. Ji, X. Song, J. Liu, Z. Yan, C. Huo, S. Zhang, M. Su, L. Liao, W. Wang, Z. Ni, Y. Hao, and H. Zeng, Two-dimensional antimonene single crystals grown by van der Waals epitaxy, *Nat. Commun.* **7**, 13352 (2016).
- [23] X. Wu, Y. Shao, H. Liu, Z. Feng, Y. L. Wang, J. T. Sun, C. Liu, J. O. Wang, Z. L. Liu, S. Y. Zhu, Y. Q. Wang, S. X. Du, Y. G. Shi, K. Ibrahim, and H. J. Gao, Epitaxial growth and air-stability of monolayer antimonene on PdTe₂, *Adv. Mater.* **29**, 1605407 (2016).
- [24] Y. Ueda, N. H. D. Khang, K. Yao, and P. N. Hai, Epitaxial growth and characterization of Bi_{1-x}Sb_x spin Hall thin films on GaAs(111)A substrates, *Appl. Phys. Lett.* **110**, 062401 (2017).
- [25] F. Reis, G. Li, L. Dudy, M. Bauernfeind, S. Glass, W. Hanke, R. Thomale, J. Schäfer, and R. Claessen, Bismuthene on a SiC substrate: A candidate for a high-temperature quantum spin Hall material, *Science* **357**, 287 (2017).
- [26] W. Yu, C.-Y. Niu, Z. Zhu, X. Cai, L. Zhang, S. Bai, R. Zhao, and Y. Jia, Strain induced quantum spin Hall insulator in monolayer β -BiSb from first-principles study, *RSC Adv.* **7**, 27816 (2017).
- [27] M. Hansen, *Constitution of Binary Alloys*, 2nd ed. (McGraw-Hill, New York, 1958).
- [28] H. Okamoto, Bi-Sb (busmuth-antimony), *J. Phase Equilib. Diffus.* **33**, 493 (2012).
- [29] D. P. Shoemaker, T. C. Chasapis, D. Do, M. C. Francisco, D. Y. Chung, S. D. Mahanti, A. Llobet, and M. G. Kanatzidis, Chemical ordering rather than random alloying in SbAs, *Phys. Rev. B* **87**, 094201 (2013).
- [30] A. Ektarawong, Y. P. Feng, and B. Alling, Phase stability of three-dimensional bulk and two-dimensional monolayer As_{1-x}Sb_x solid solutions from first principles, *J. Phys.: Condens. Matter* **31**, 245702 (2019).
- [31] J. M. Sanchez, F. Ducastelle, and D. Gratias, Generalized cluster description of multicomponent systems, *Physica A (Amsterdam)* **128**, 334 (1984).
- [32] A. van de Walle and G. Ceder, Automating first-principles phase diagram calculations, *J. Phase Equilib.* **23**, 348 (2002).
- [33] A. van de Walle, M. Asta, and G. Ceder, The alloy theoretic automated toolkit: A user guide, *CALPHAD J.* **26**, 539 (2002).
- [34] P. E. Blöchl, Projector augmented-wave method, *Phys. Rev. B* **50**, 17953 (1994).
- [35] G. Kresse and J. Furthmüller, Efficiency of ab-initio total energy calculations for metals and semiconductors using a plane-wave basis set, *Comput. Mater. Sci.* **6**, 15 (1996).
- [36] G. Kresse and J. Furthmüller, Efficient iterative schemes for *ab initio* total-energy calculations using a plane-wave basis set, *Phys. Rev. B* **54**, 11169 (1996).
- [37] J. Perdew, K. Burke, and M. Ernzerhof, Generalized Gradient Approximation Made Simple, *Phys. Rev. Lett.* **77**, 3865 (1996).
- [38] H. J. Monkhorst and J. D. Pack, Special points for Brillouin-zone integrations, *Phys. Rev. B* **13**, 5188 (1976).
- [39] S. Grimme, J. Antony, S. Ehrlich, and S. Kreig, A consistent and accurate *ab initio* parametrization of density functional dispersion correction (DFT-D) for the 94 elements H-Pu, *J. Chem. Phys.* **132**, 154104 (2010).
- [40] G. Kresse and O. Lebacqz, VASP manual, <http://cms.mpi.univie.ac.at/vasp/>
- [41] D. Hobbs, G. Kresse, and J. Hafner, Fully unconstrained noncollinear magnetism within the projector augmented-wave method, *Phys. Rev. B* **62**, 11556 (2000).
- [42] P. E. Blöchl, O. Jepsen, and O. K. Andersen, Improved tetrahedron method for brillouin-zone integrations, *Phys. Rev. B* **49**, 16223 (1994).
- [43] A. van de Walle and M. Asta, Self-driven lattice-model Monte Carlo simulations of alloy thermodynamics properties and phase diagrams, *Model. Simul. Mater. Sci. Eng.* **10**, 521 (2002).
- [44] G. L. W. Hart and R. W. Forcade, Algorithm for generating derivative structures, *Phys. Rev. B* **77**, 224115 (2008).
- [45] A. Zunger, S.-H. Wei, L. G. Ferreira, and J. E. Bernard, Special Quasirandom Structures, *Phys. Rev. Lett.* **65**, 353 (1990).
- [46] A. V. Ruban and I. A. Abrikosov, Configurational thermodynamics of alloys from first principles: Effective cluster interactions, *Rep. Prog. Phys.* **71**, 046501 (2008).
- [47] A. Ektarawong, S. I. Simak, and B. Alling, Carbon-rich icosahedral boron carbides beyond B₄C and their thermodynamic stabilities at high temperature and pressure from first principles, *Phys. Rev. B* **94**, 054104 (2016).
- [48] A. Ektarawong, S. I. Simak, and B. Alling, Effect of temperature and configurational disorder on the electronic band gap of boron carbide from first principles, *Phys. Rev. Mater.* **2**, 104603 (2018).
- [49] G. Oelgart, G. Schneider, W. Kraak, and R. Herrmann, The semiconductor-semimetal transition in Bi_{1-x}Sb_x alloys, *Phys. Status Solidi B* **74**, K75 (1976).
- [50] W. Kraak, G. Oelgart, G. Schneider, and R. Herrmann, The semiconductor-semimetal transition in Bi_{1-x}Sb_x alloys with $x \geq 0.22$, *Phys. Status Solidi B* **88**, 105 (1978).
- [51] B. Lenoir, A. Dauscher, M. Cassart, Yu. I. Ravich, and H. Scherrer, Effect of antimony content on the thermoelectric figure of merit of Bi_{1-x}Sb_x alloys, *J. Phys. Chem. Solids* **59**, 129 (1998).
- [52] S. Cho, Y. Kim, A. DiVenere, G. K. L. Wong, A. J. Freeman, J. B. Ketterson, L. J. Olafsen, I. Vurgaftman, J. R. Meyer, and C. A. Hoffman, Artificially ordered BiSb alloys: Growth and transport properties, in *Eighteenth International Conference on Thermoelectrics. Proceedings, ICT'99 (Cat. No. 99TH8407)* (IEEE, Piscataway, NJ, 1999), p. 104.